Polyphenol-Binding Amyloid Fibrils Self-Assemble Into Reversible Hydrogels With Antibacterial Activity

Bing Hu[†,‡*], Yang Shen[§], Jozef Adamcik[‡], Peter Fischer[¶], Mirjam Schneider[#], Martin J. Loessner[§], Raffaele Mezzenga[‡*]

[†]College of Food Science and Technology, Nanjing Agricultural University, 1 Weigang, Nanjing, Jiangsu, 210095 P. R. China.

[‡]Laboratory of Food and Soft Materials, Department of Health Sciences and Technology, ETH Zurich, Schmelzbergstrasse 9, 8092 Zurich, Switzerland.

[§]Laboratory of Food Microbiology, Department of Health Sciences and Technology, ETH Zurich, Schmelzbergstrasse 7, 8092 Zurich, Switzerland.

[¶]Laboratory of Food Process Engineering, Department of Health Sciences and Technology, ETH Zurich, Schmelzbergstrasse 7, 8092 Zurich, Switzerland.

[#]Laboratory of Toxicology, Department of Health Sciences and Technology, ETH Zurich, Schmelzbergstrasse 9, 8092 Zurich, Switzerland.

*To whom correspondence should be addressed.

Email: hubing212002@njau.edu.cn; raffaele.mezzenga@hest.ethz.ch

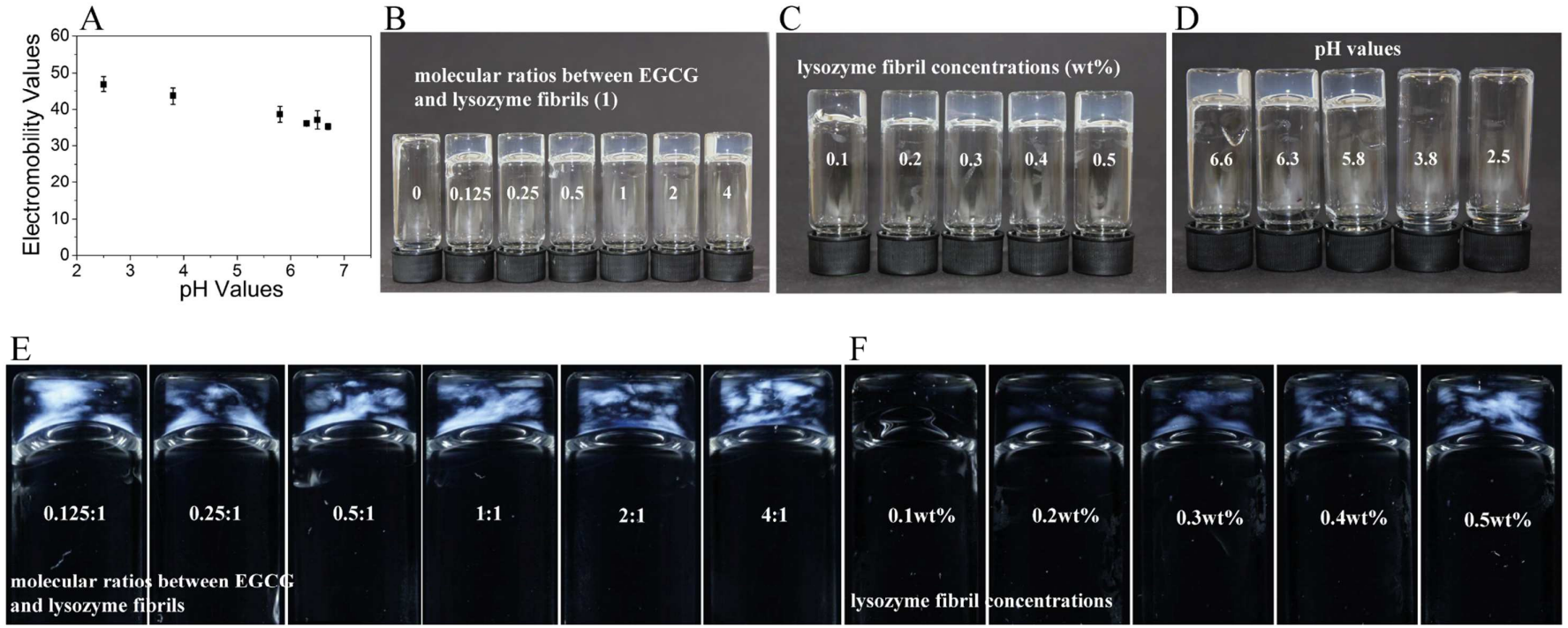

Figure S1. Formation of lysozyme amyloid fibrils and the polyphenol induced fibril hydrogels. (A) The linear charge density of lysozyme fibrils under different pH values. (B) Incubation of EGCG with lysozyme fibrils (0.5 wt%) with different molecular ratios between EGCG and lysozyme fibril for 72 hours at pH 5.8. (C) Incubation of EGCG with lysozyme fibrils under different fibrils concentrations with fixed molecular ratio between EGCG and lysozyme fibril of 4:1 for 96 hours at pH 5.8. (D) Incubation of EGCG with lysozyme fibrils under different pH values with fixed fibrils concentration of 0.2 wt%, and fixed molecular ratio between EGCG and lysozyme fibril of 4:1 for 120 hours. Upturn tests and birefringence of the samples of incubating EGCG with lysozyme fibrils (0.5 wt%) under different molecular ratios between EGCG and lysozyme fibrils for 72 hours at pH 5.8 (E); and incubation of EGCG with lysozyme fibrils at different fibril concentrations with fixed molecular ratio between EGCG and lysozyme fibril of 4:1 for 96 hours at pH 5.8 (F).

The hydrogels formed with different molecular ratio of EGCG to lysozyme fibrils after incubation for 72 hours are shown in Figure S1B, which exhibit birefringence under polarized light (Figure S1E). However, lysozyme fibrils without EGCG could not form hydrogel (Figure S1B). With the fixed molecular ratio between EGCG and lysozyme fibrils at 4:1, hydrogels can form in the tested fibril concentration range of 0.1 to 0.5 wt% after incubation for 12 hours. Figure S1C shows the picture of hydrogels formed with different fibril concentrations after incubation for 96 hours. Birefringence of the hydrogels enhances with increase of fibril concentrations (Figure S1F). At pH 2.5 and 3.8, EGCG fails to induce fibril hydrogels even after incubation for 120 hours (Figure S1D). In relative high pH environments (pH 5.8 to 6.7), EGCG induces formation of the hydrogels (Figure S1D).

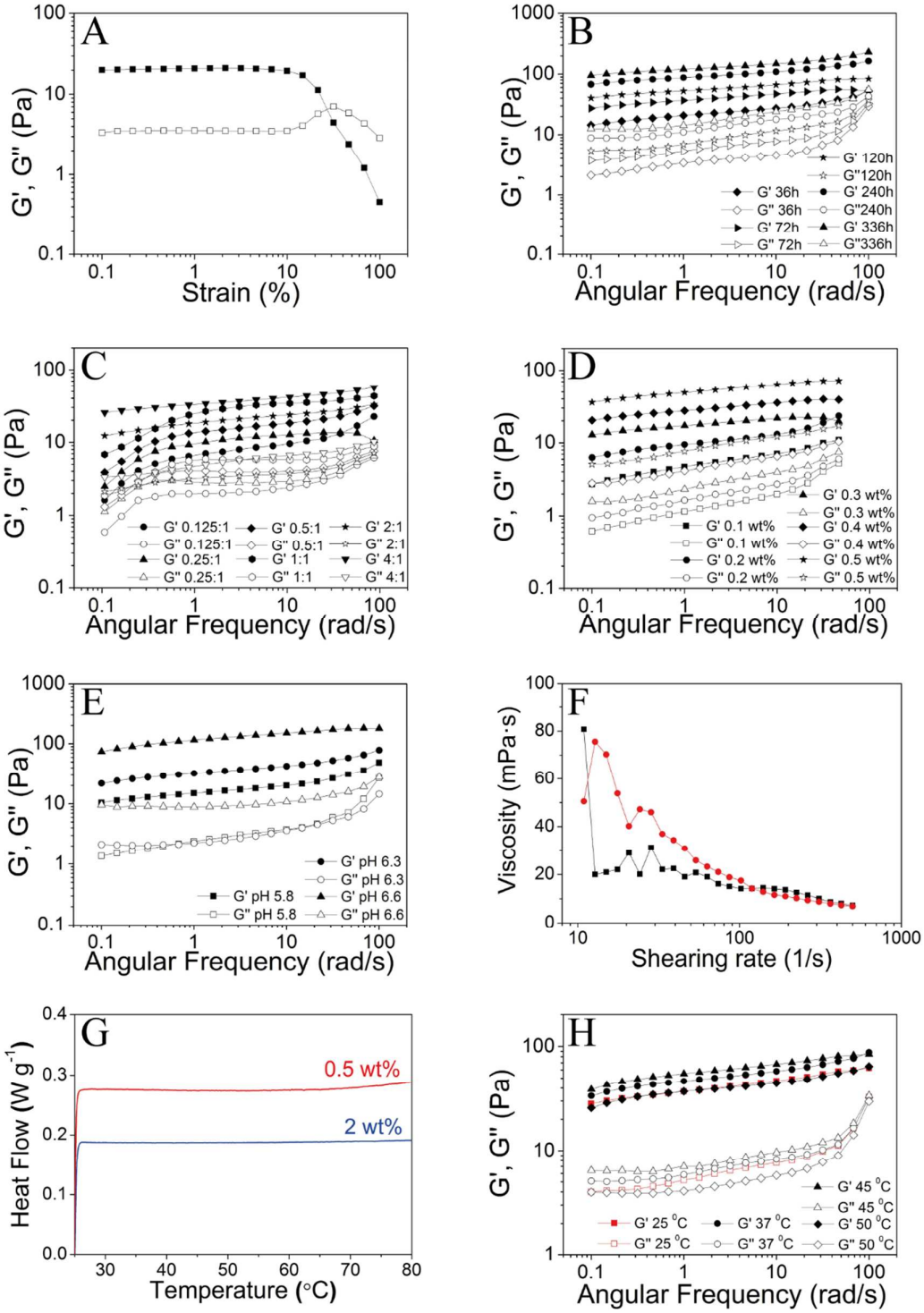

Figure S2. Characterization of the polyphenol induced lysozyme amyloid fibril hydrogels. (A) Strain dependence of the storage (G', filled symbols) and loss (G'', open symbols) moduli of the hydrogel sample measured at a fixed frequency of 1 rad/s (The hydrogels form after incubation of lysozyme fibrils with EGCG for 12h, with the molecular ratio between EGCG and lysozyme fibril of 4:1, at pH 5.8). Frequency dependence of the storage modulus (G',

filled symbols) and loss modulus (G'', open symbols) of the samples at (B) different incubation time of 36, 72, 120, 240 and 336h with the molecular ratio between EGCG and lysozyme fibril of 4:1 and the fibril concentration of 0.5 wt% at pH 5.8; (C) different molecular ratios between EGCG and amyloid fibril of 0.125:1, 0.25:1, 0.5:1, 1:1, 2:1 and 4:1 with the fibril concentration of 0.5 wt% and incubation time of 72h at pH 5.8; (D) different fibril concentrations of 0.1, 0.2, 0.3, 0.4, and 0.5 wt% with the molecular ratio between EGCG and lysozyme fibril of 4:1 and the incubation time of 96h at pH 5.8; (E) under different pH values of pH5.8, pH6.3 and pH6.6 with fibril concentration of 0.2 wt%, molecular ratio between EGCG and lysozyme fibril of 4:1 and the incubation time of 120h. (F) Flow curve from low to high shear rates (black symbols, 10 to 500 s^{-1}) and back at high to low shear rates (red symbols, 500 to 10 s^{-1}). (G) DSC thermogram of the EGCG induced lysozyme fibril hydrogels with the fibril concentration of 0.5 wt% and 2 wt% (heating rate of $dT/dt = 1$ K min^{-1}, 40 μL aluminum crucibles under N_2 atmosphere). (H) Frequency dependence of the storage modulus (G', filled symbols) and loss modulus (G'', open symbols) for the hydrogels induced by incubation of lysozyme fibrils (0.5 wt%) with EGCG with the molecular ratio between EGCG and lysozyme fibril of 4:1 and the incubation time of 72h at pH 5.8 at different temperatures of 25, 37, 45 and 50 °C.

Rheology measurements confirmed formation of the hydrogels and characterized the effects of different parameters on hydrogel viscoelastic properties. Strain of 1% used in the frequency sweeping measurement is in the linear viscoelastic regime of hydrogels as shown in amplitude oscillatory shear (Figure S2A). For the samples shown in Figure S2B, the storage modulus G' is approximately independent of frequency, and dominates the loss modulus G'' for approximate one order of magnitude within the entire frequency range, which indicates a typical gel-like behavior. Both G' and G'' of the hydrogels increase gradually with prolonged incubation time from 36 hours to 2 weeks (Figure S2B). Figure S2C shows the impact of molecular ratio between EGCG and lysozyme fibrils on hydrogel viscoelastic properties. After incubation for 72 hours, for molecular ratios ≤ 1, G' increases with frequency from 0.1 to 1 rad/s. For molecular ratio ≥ 2, G' becomes approximately independent of frequency and increases with the molecular ratio. This result indicates that increasing content of EGCG in the mixture system promotes formation of the hydrogels. Positive correlation between G' and fibril concentration is shown in Figure S2D. The strength of the hydrogels is also positively related to pH values (Figure S2E). In highly acidic environments, strong repulsion among

fibrils could inhibit formation of the fibril networks (Figure S1D). With increase of pH values, the linear charge density of fibrils decreases, resulting in the formation of hydrogels and enhanced gel strength. The hydrogels' viscosity decreases with the increase of shear rate from 10 to 500 1/s, and recovers as the shear rate reverses from 500 to 10 1/s (Figure S2F). This indicates that the EGCG induced fibril hydrogels are shear thinning and reversible.

In order to investigate the thermal stability of the EGCG induced lysozyme fibril hydrogels, heating of hydrogels at different temperatures was carried out. Figure S3 shows that, the hydrogels do not flow or melt and can withstand an upturn test after heating for 30 min under different temperatures from 25 to 90 ^{0}C. In addition, differential scanning calorimetry (DSC) results do not show any phase transition in the range from 25 to 90 °C, in either 0.5 or 2 wt% fibril concentration hydrogels (Figure S2G). Therefore, the hydrogels are thermally resistant. Furthermore, hydrogel viscoelasticity was characterized by rheology measurements carried out at increasing temperatures from 25 to 50 ^{0}C, and temperature was not found to significantly influence the frequency behavior (Figure S2H). Temperatures higher than 50 ^{0}C were not considered due to potential water evaporation, despite the solvent trap used.

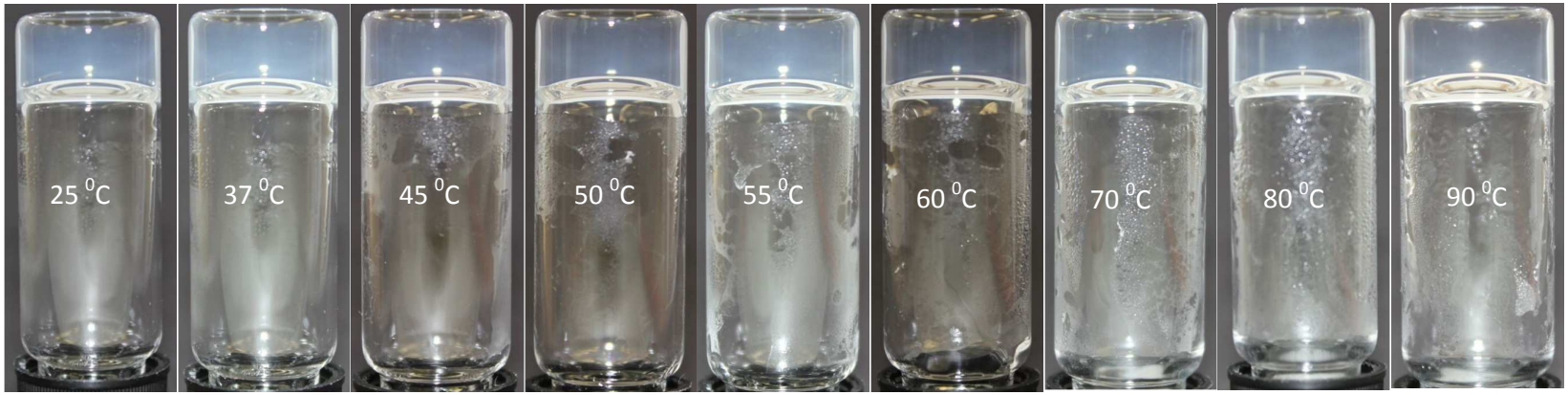

Figure S3. Upturn tests of the EGCG induced lysozyme fibril hydrogels after heating for 30 min under different temperatures from 25 to 90^{0}C.

Figure S4. Upturn tests (A) and birefringence (B) of the samples of incubating morin with lysozyme fibrils (0.5 wt%) under different molecular ratios between morin and lysozyme fibrils for 12 hours under pH 5.8.

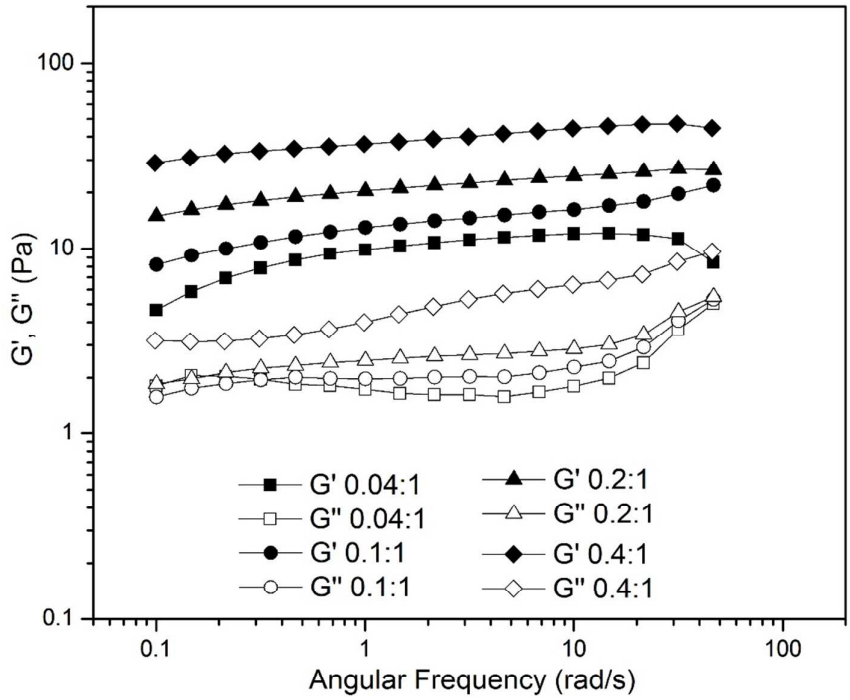

Figure S5. Frequency dependence of the storage modulus (G', filled symbols) and loss modulus (G'', open symbols) of the hydrogels at different molecular ratios between morin and lysozyme amyloid fibrils with the fibril concentration of 0.5 wt% and incubation time of 96h.

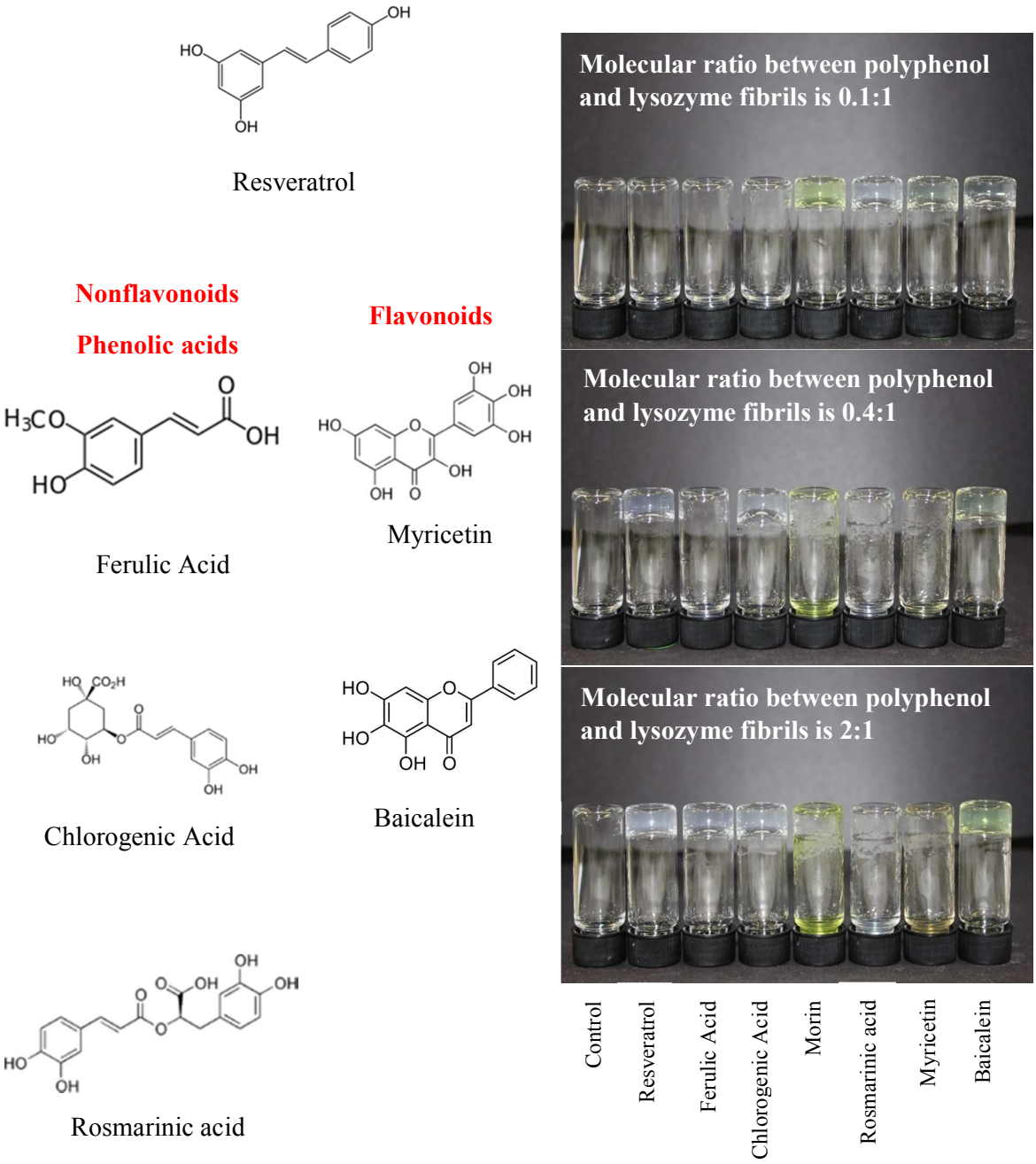

Figure S6. Formation of the lysozyme fibrils hydrogels after incubation of the fibrils with different polyphenols under different molecular ratio between the polyphenol and the fibrils.

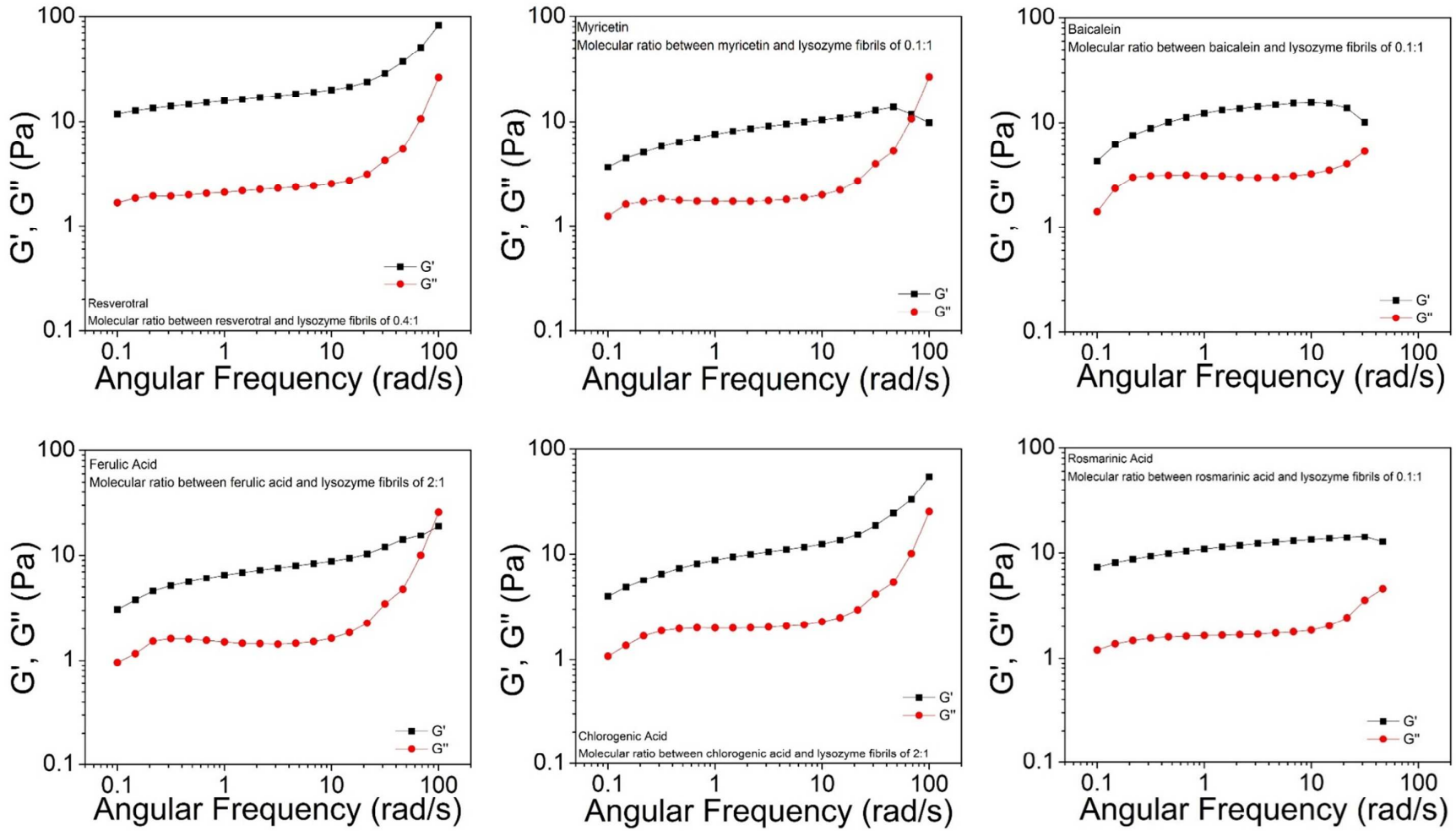

Figure S7. Frequency dependence of the storage modulus (G', filled symbols) and loss modulus (G'', open symbols) of the polyphenols induced lysozyme fibril hydrogels.

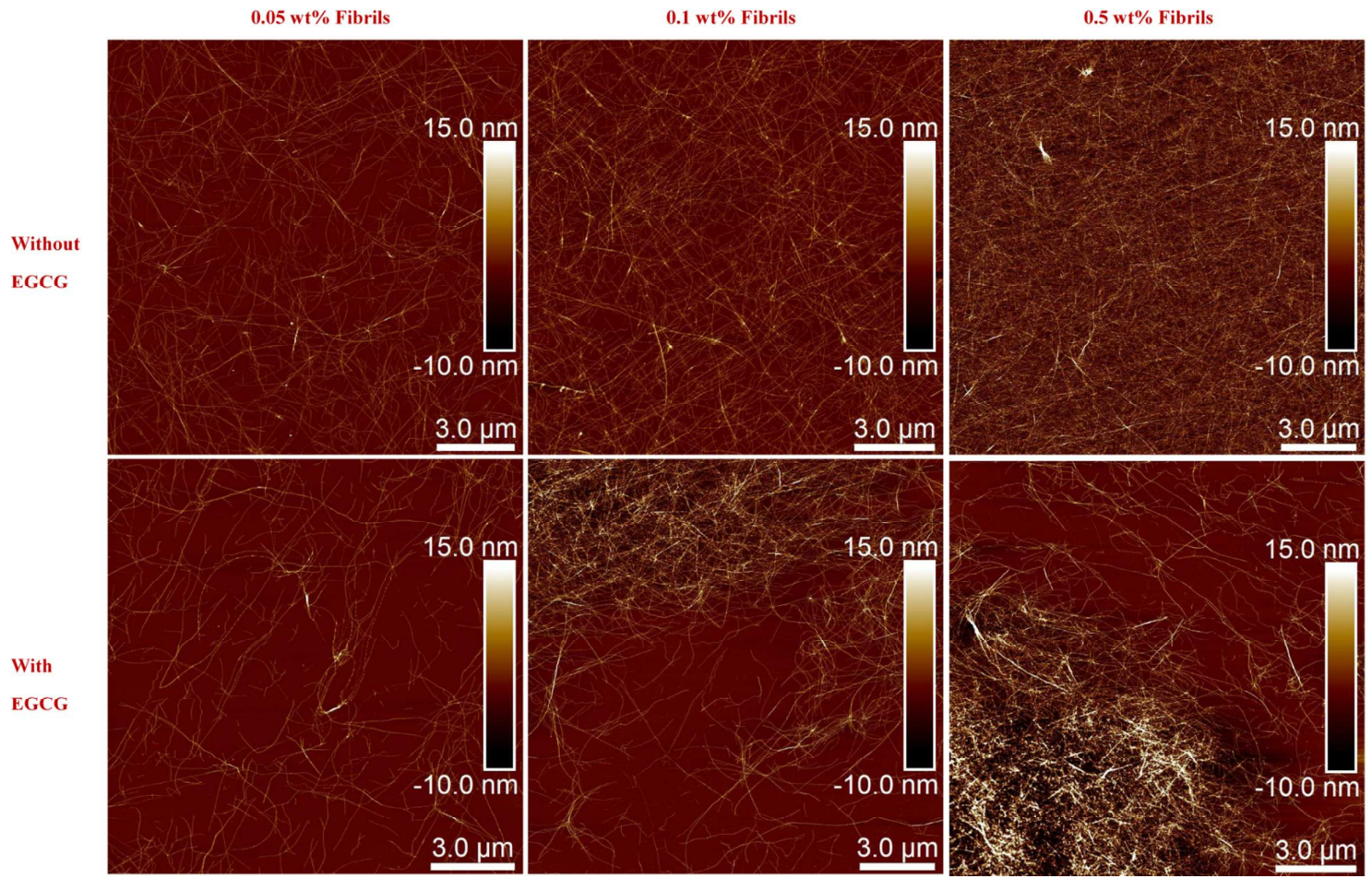

Figure S8. Behavior of the lysozyme amyloid fibrils with different concentrations induced by the polyphenol in microscopic scale. The AFM images of the morphology of lysozyme fibrils incubated with or without (−)-epigallocatechin-3-gallate (EGCG) with different fibril concentrations of 0.05, 0.1 and 0.5 wt%, the fixed molecular ratio between EGCG and lysozyme fibril of 4:1, and incubation time of 24 hours at pH 5.8.

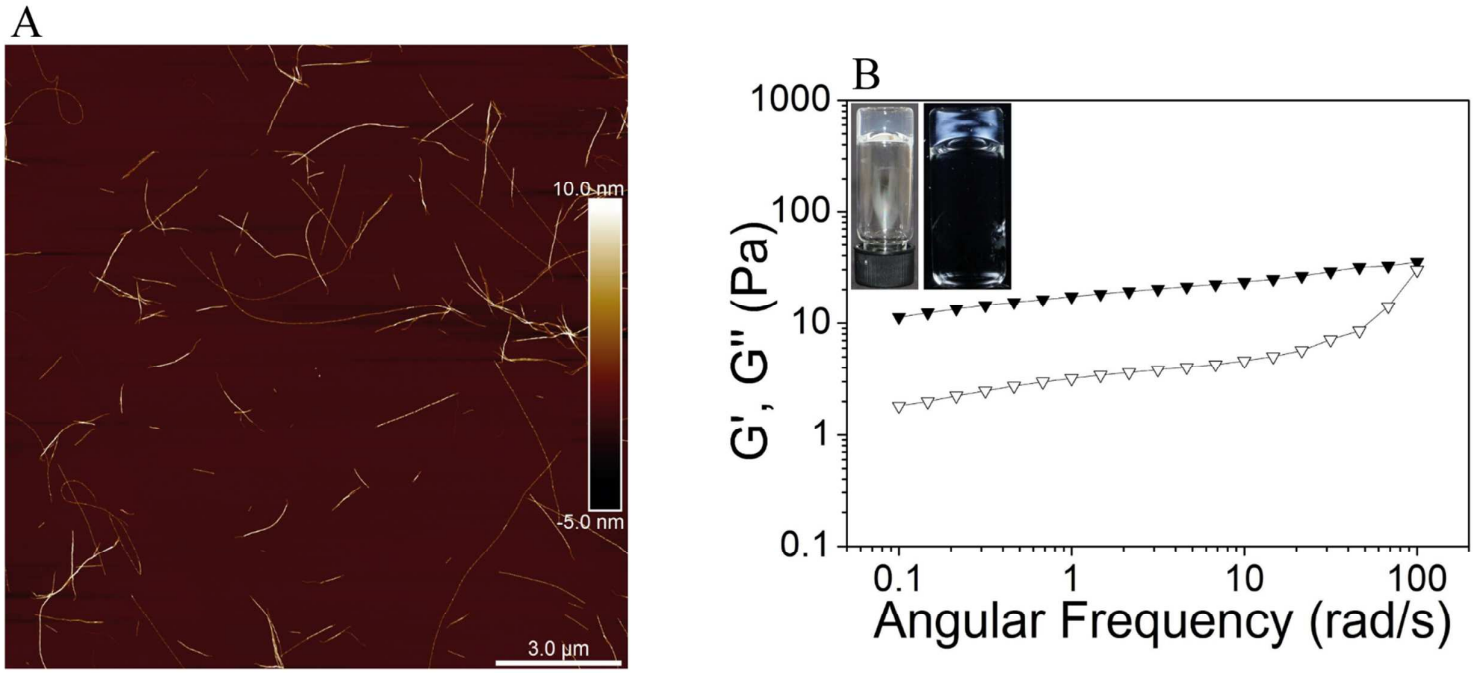

Figure S9. Formation of the lysostaphin M23 endopeptidase amyloid fibrils and the polyphenol induced fibril hydrogels. (A) The AFM images of the morphology of lysostaphin M23 endopeptidase amyloid fibrils in pH2 water at fibril concentration of 0.005 wt%. (B) Frequency dependence of the storage modulus (G', filled symbols) and loss modulus (G'', open symbols) of the EGCG induced lysostaphin M23 endopeptidase amyloid fibril hydrogels with incubation time of 36h, the molecular ratio between EGCG and the fibril of 4:1 and the fibril concentration of 0.5 wt% at pH 5.8 (inserts are the pictures of the hydrogels under daylight and polarized light).

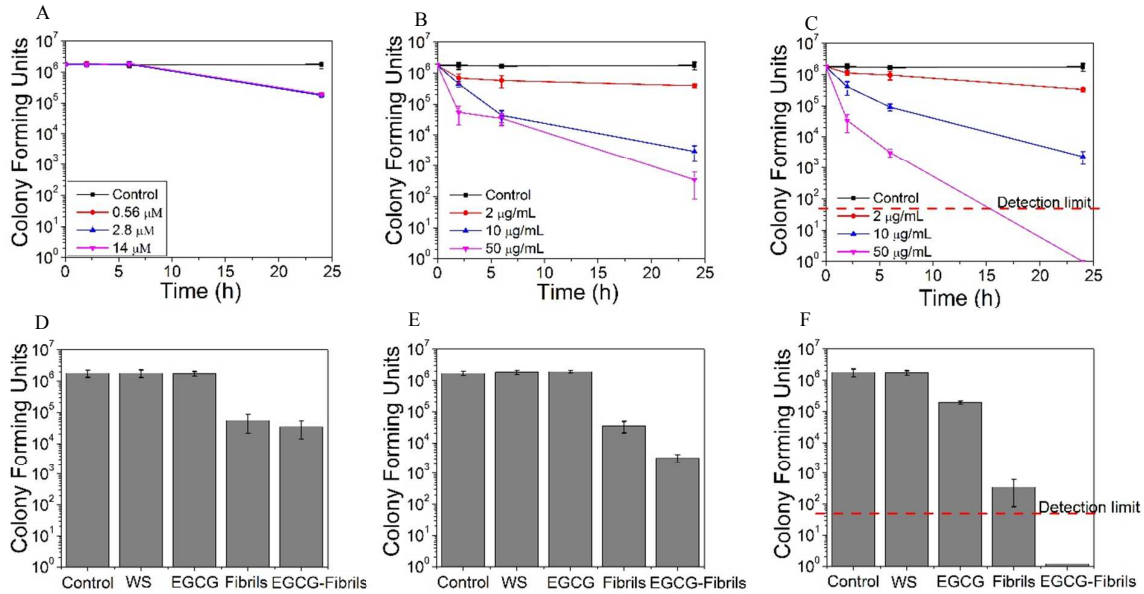

Figure S10. Time and concentration dependency for reducing colony-forming unit (CFU) of *E. coli* by EGCG (A), lysozyme fibrils (B) and EGCG-binding lysozyme fibrils (C) with the concentration in term of the fibrils. Effect on reducing CFU of *E. coli* after 2h (D), 6h (E), and 24 h (F) exposure to EGCG-binding fibrils (50 μg/mL lysozyme fibrils and 14 μM EGCG), lysozyme fibirls (50 μg/mL), EGCG (14 μM), blank working solution, and Bis-Tris buffer (control).

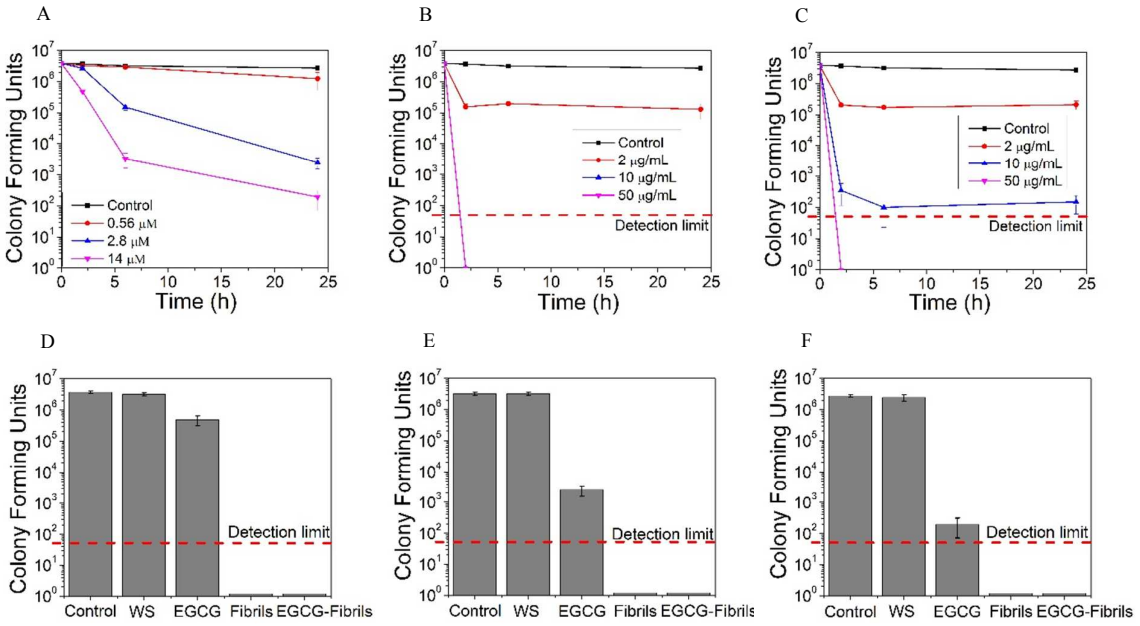

Figure S11. Time and concentration dependency for reducing colony-forming unit (CFU) of *Listeria monocytogenes* WSLC 1042 by EGCG (A), lysozyme fibrils (B) and EGCG-binding lysozyme fibrils (C) with the concentration in term of the fibrils. Effect on reducing CFU of *Listeria monocytogenes* after 2h (D), 6h (E), and 24 h (F) exposure to EGCG-binding fibrils (50 μg/mL lysozyme fibrils and 14 μM EGCG), lysozyme fibrils (50 μg/mL), EGCG (14 μM), blank working solution, and Bis-Tris buffer (control).

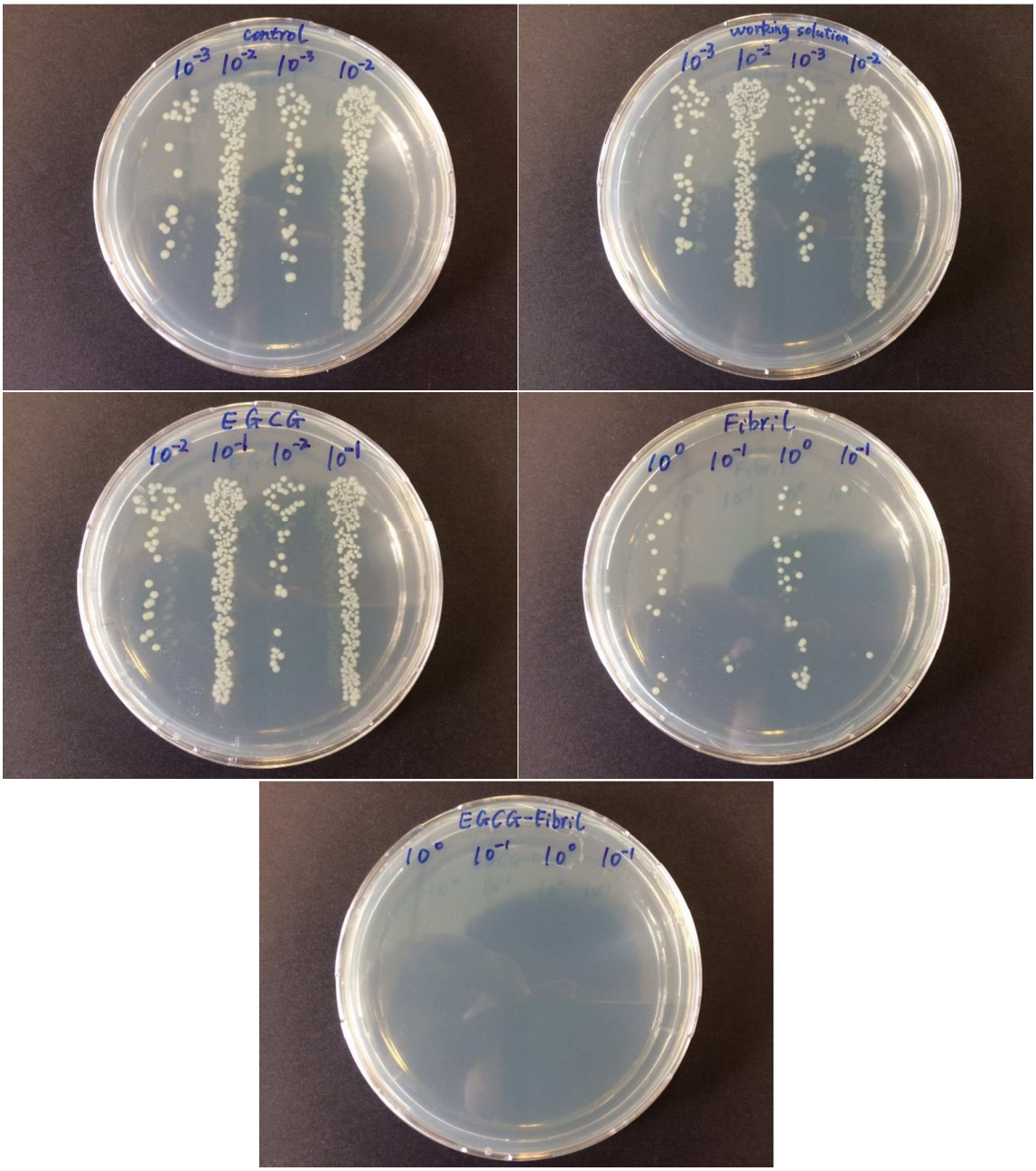

Figure S12. Time and concentration dependency for reducing colony-forming unit (CFU) of *E. coli* K12 after 24 h exposure to EGCG-binding fibrils (50 μg/mL lysozyme fibrils and 14 μM EGCG), lysozyme fibrils (50 μg/mL), EGCG (14 μM), blank working solution, and Bis-Tris buffer (control).

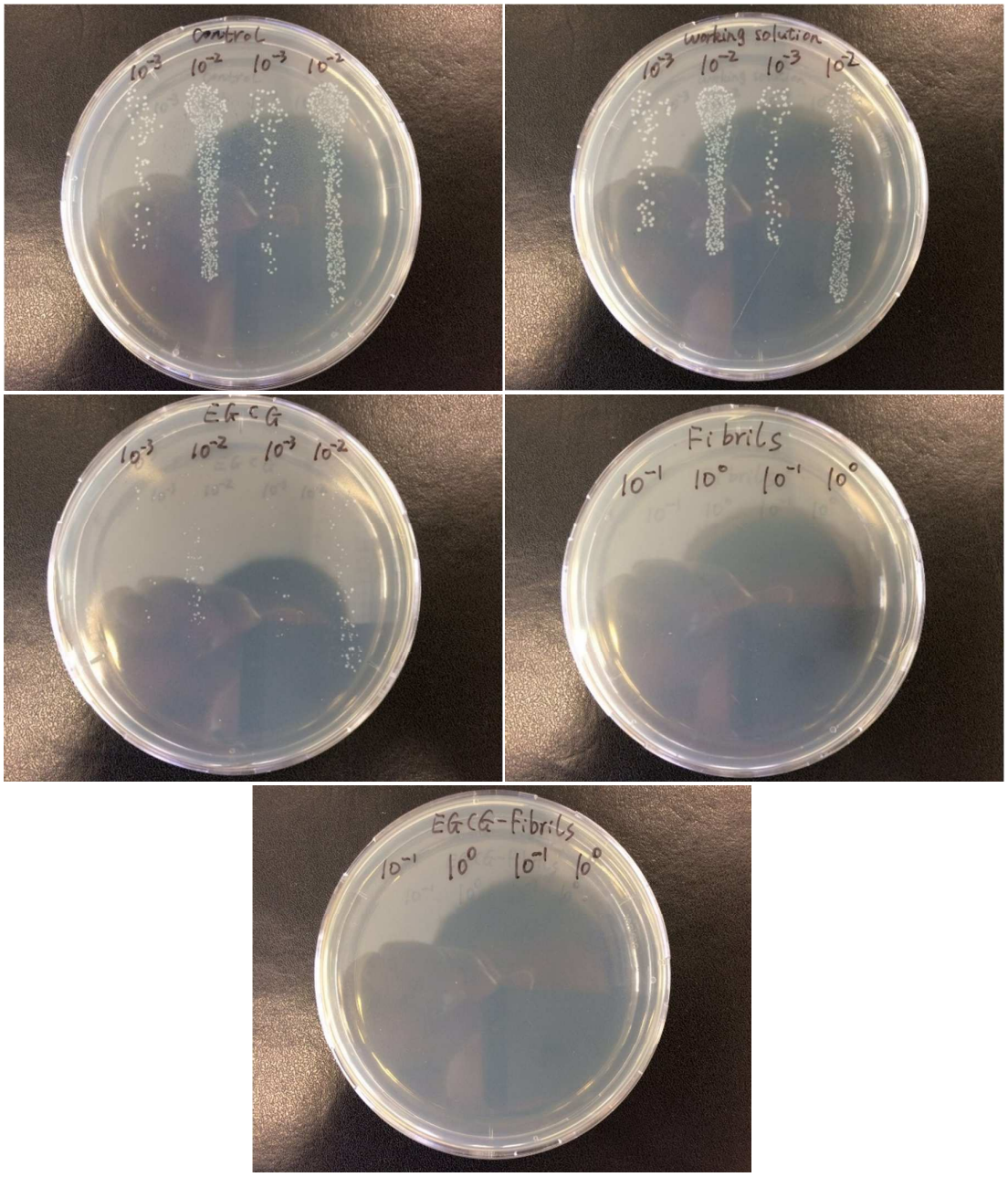

Figure S13. Time and concentration dependency for reducing colony-forming unit (CFU) of *Listeria monocytogenes* WSLC 1042 after 2 h exposure to EGCG-binding fibrils (50 μg/mL lysozyme fibrils and 14 μM EGCG), lysozyme fibrils (50 μg/mL), EGCG (14 μM), blank working solution, and Bis-Tris buffer (control).

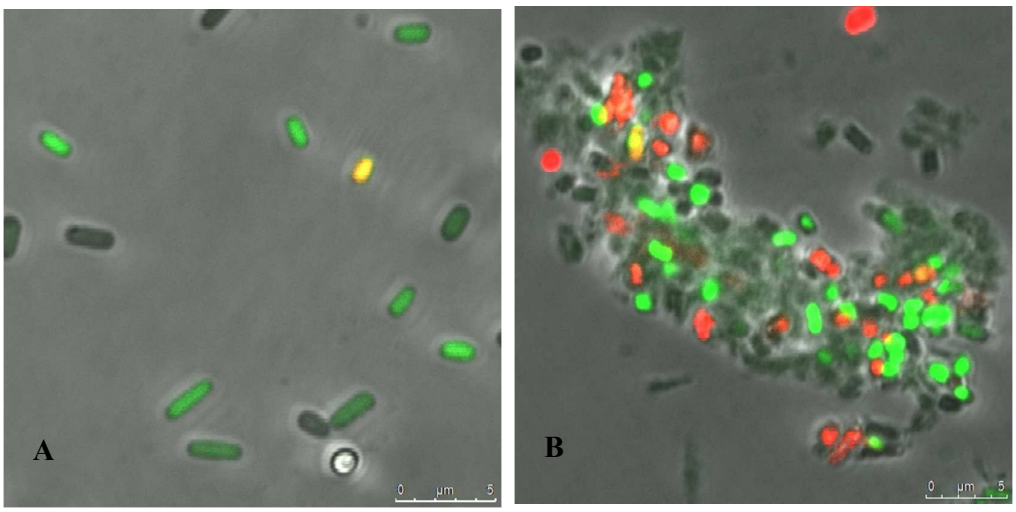

Figure S14. CLSM images of *E. coli* incubated with buffer (A) and the salt induced lysozyme fibril hydrogels (B), respectively, for 30 min by LIVE/DEAD BacLight bacterial viability assay.

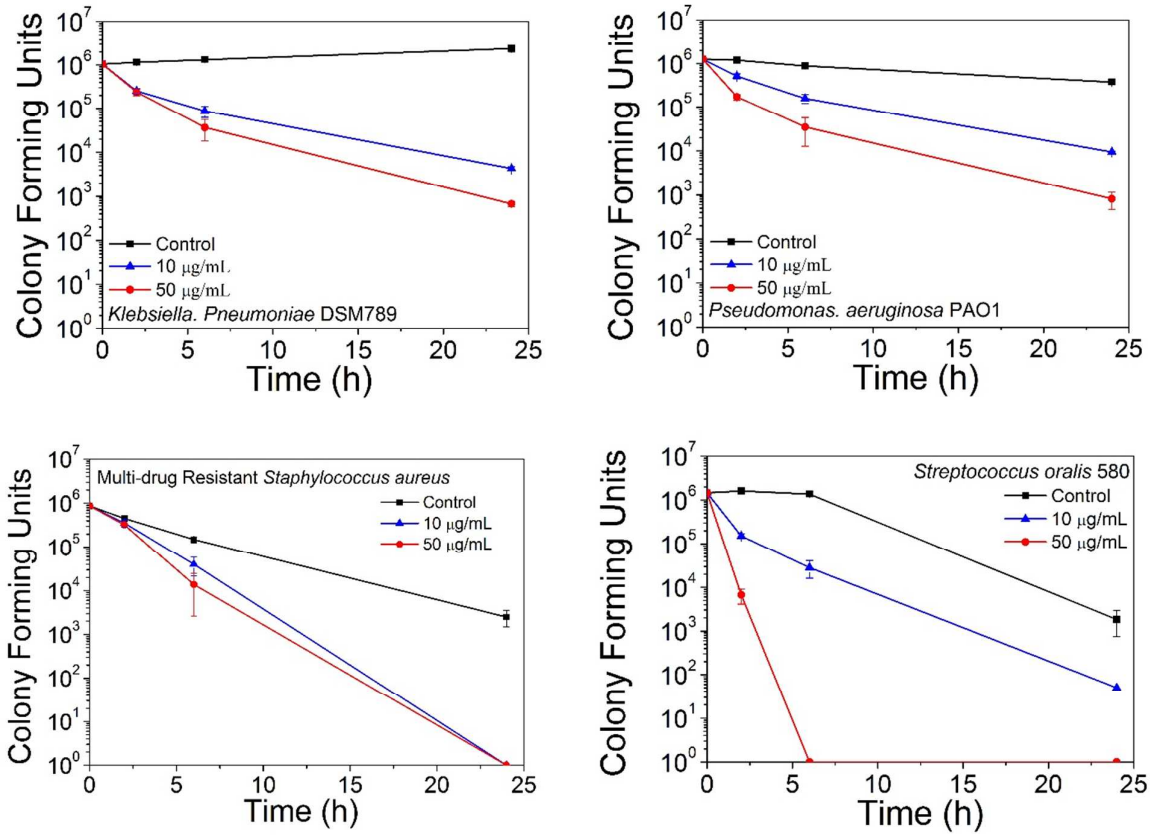

Figure S15. Time and concentration dependency for reducing colony-forming unit (CFU) of *Klebsiella pneumoniae* DSM789, *Pseudomonas aeruginosa* PAO1, Clinically isolated methicillin-resistant *Staphylococcus aureus* ZH124, and *Streptococcus oralis* 580 by lysozyme amyloid fibrils.

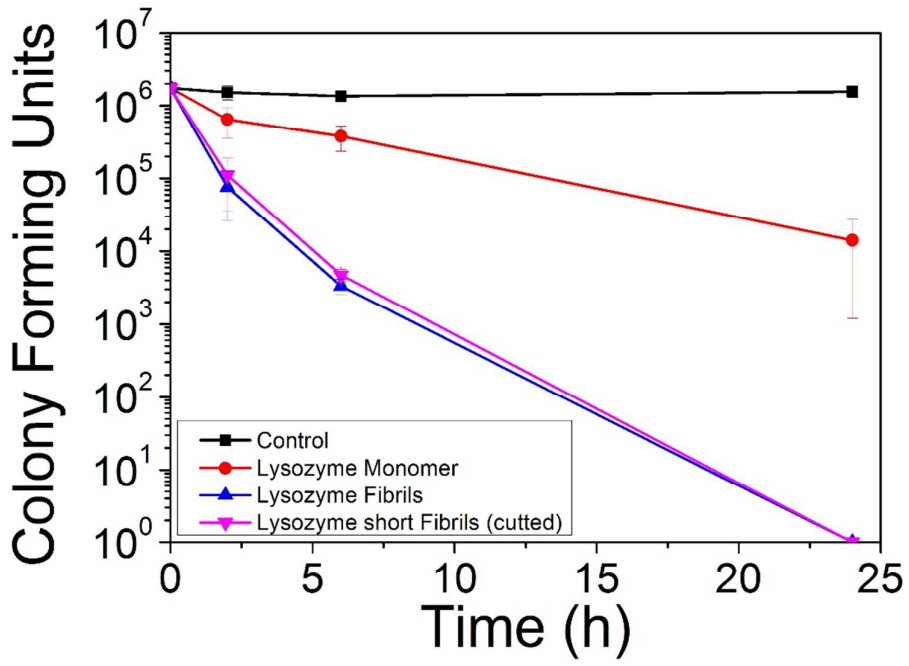

Figure S16. Time and concentration dependency for reducing colony-forming unit (CFU) of *E. Coli* K12 by native lysozyme protein monomer, mature fibrils and the cutted short fibrils at the same protein concentration of 50 μg/mL.

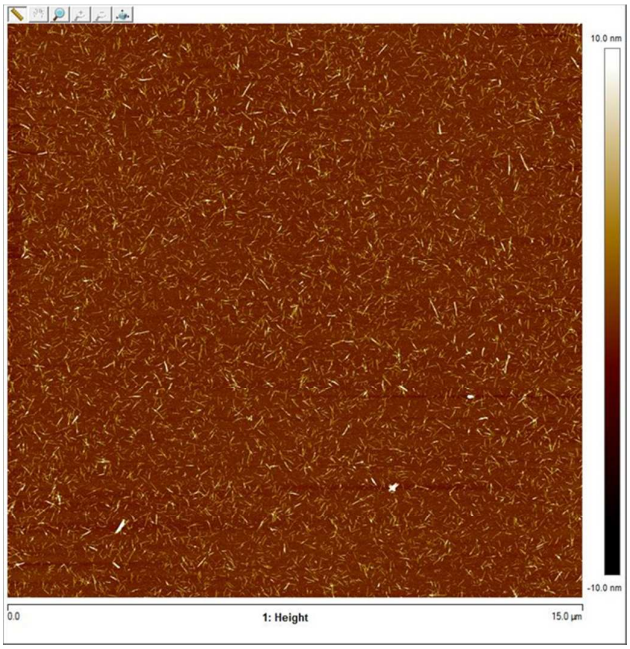

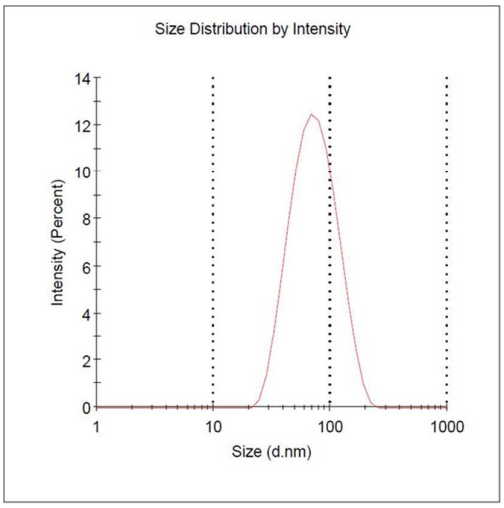

Average Size: 62.58 ± 27.10 nm
Polydispersity Index: 0.188
Zeta Potential: 39.7 mV

Figure S17. The AFM image (A) and size distribution (B, measure by dynamic light scattering) of the cutted short lysozyme fibrils.